TISSUE ENGINEERING: Part A
Volume 15, Number 5, 2009

DOI: 10.1089/ten.tea.2008.0099

Differential Maturation and Structure–Function Relationships in Mesenchymal Stem Cell- and Chondrocyte-Seeded Hydrogels

Isaac E. Erickson, B.S.,[1,2] Alice H. Huang, B.S.,[1,2] Cindy Chung, B.S.,[2] Ryan T. Li, B.S.,[1] Jason A. Burdick, Ph.D.,[2] and Robert L. Mauck, Ph.D.[1,2]

Degenerative disease and damage to articular cartilage represents a growing concern in the aging population. New strategies for engineering cartilage have employed mesenchymal stem cells (MSCs) as a cell source. However, recent work has suggested that chondrocytes (CHs) produce extracellular matrix (ECM) with superior mechanical properties than MSCs do. Because MSC–biomaterial interactions are important for both initial cell viability and subsequent chondrogenesis, we compared the growth of MSC- and CH-based constructs in three distinct hydrogels—agarose (AG), photocrosslinkable hyaluronic acid (HA), and self-assembling peptide (Puramatrix, Pu). Bovine CHs and MSCs were isolated from the same group of donors and seeded in AG, Pu, and HA at 20 million cells/mL. Constructs were cultured for 8 weeks with biweekly analysis of construct physical properties, viability, ECM content, and mechanical properties. Correlation analysis was performed to determine quantitative relationships between formed matrix and mechanical properties for each cell type in each hydrogel. Results demonstrate that functional chondrogenesis, as evidenced by increasing mechanical properties, occurred in each MSC-seeded hydrogel. Interestingly, while CH-seeded constructs were strongly dependent on the 3D environment in which they were encapsulated, similar growth profiles were observed in each MSC-laden hydrogel. In every case, MSC-laden constructs possessed mechanical properties significantly lower than those of CH-seeded AG constructs. This finding suggests that methods for inducing MSC chondrogenesis have yet to be optimized to produce cells whose functional matrix-forming potential matches that of native CHs.

Introduction

Articular cartilage lines the bony surfaces of joints and functions to transmit the high stresses that arise with joint motion.[1] The tissue extracellular matrix (ECM) is comprised of a dense network of collagen fibers (mainly type II) interspersed with large proteoglycan aggregates.[2] These structural elements provide for a remarkable resilience of the tissue. Chondrocytes (CHs) reside within the ECM[3] and, through their biosynthetic activities, maintain and remodel the tissue in response to its changing mechanical environment.[4,5] As a consequence of its unique mechanical properties and continual remodeling, cartilage can function in its demanding environment over a lifetime of use, though trauma or other degenerative processes can impair function. The growing prevalence of osteoarthritis, other degenerative cartilage diseases, and traumatic injuries motivates our goal of developing replacement cartilage tissue.

To address this need, tissue engineering (TE) strategies have focused on the production of functional cartilage constructs that possess features similar to the native tissue (for review, see Hung *et al.*[6] and Kuo *et al.*[7]). While it is not yet clear whether an engineered construct must completely recapitulate all mechanical features of the native tissue at the time of implantation, it is clear that if permanent biologic repair is to be effected, the engineered systems must enable this eventuality. Most cartilage TE strategies combine mature CHs with biocompatible and/or biodegradable 3D culture systems (for review, see Chung and Burdick[8]). Hydrogels, in particular, force encapsulated cells to assume a rounded shape and aid in the retention or resumption of the CH phenotype.[9,10] A large number of hydrogels have been developed for these applications, ranging from simple thermoreversible gels (such as agarose [AG]),[11] to more complex bioengineered gels that present ECM relevant adhesive (i.e., arginine-glycine-aspartic acid [RGD])[12,13] and/or degradation cues (e.g., matrix metalloproteinase (MMP)-cleavable elements).[14,15]

In many cartilage TE efforts, primary or culture-expanded CHs are employed. These cells, while possessing the proper phenotype, are of limited supply. Further limiting clinical use, aged and/or osteoarthritic CHs produce ECM lower in collagen content than young CHs do.[16,17] This, coupled with

[1]McKay Orthopaedic Research Laboratory, Department of Orthopaedic Surgery, University of Pennsylvania, Philadelphia, Pennsylvania.
[2]Department of Bioengineering, University of Pennsylvania, Philadelphia, Pennsylvania.

in vitro expansion–induced CH dedifferentiation,[18,19] has initiated new efforts on the use of adult-derived mesenchymal stem cells (MSCs). MSCs can be isolated from adult bone marrow, and possess a multilineage differentiation capacity.[20–22] In pellet cultures in defined media supplemented with TGFβ/BMP superfamily members,[23] MSCs undergo chondrogenesis and deposit a proteoglycan-rich ECM.[24] This same phenotypic conversion has been demonstrated in a number of hydrogels.[25–28] However, while MSC chondrogenesis is apparent at the molecular/histological level, few studies have evaluated the resultant mechanical properties developed in these MSC-laden constructs or compared them directly to those achieved by CHs. In one study using adipose-derived adult stem (ADAS) cells, the mechanical properties of cell-laden AG, alginate, and fibrous gelatin–based foams were evaluated over a 4-week time course.[27] In that study, mechanical properties increased modestly with time, but primary CH controls were not examined. More recently, we acquired bovine CHs and MSCs from the same donor or groups of healthy donors and evaluated their maturation with long-term culture in AG in a pro-chondrogenic media formulation.[24,29] Testing the equilibrium and dynamic mechanical properties of these constructs showed that while MSC-laden constructs increased in mechanical properties, they did so to a lesser extent than CH-laden constructs.

MSC–biomaterial interactions are important for both initial viability and subsequent chondrogenesis. For example, human MSCs decrease in viability in hydrogels when not presented with the appropriate 3D adhesive niche.[30,31] MSCs can be isolated based on their adhesion to tissue culture plastic, and thus precipitating the first step in phenotypic conversion may be necessary to maintain viability in this anchorage-dependent population. Conversely, these same adhesive cues may negatively regulate chondrogenic differentiation; a recent study showed that RGD-modified alginate decreased the extent of MSC chondrogenesis as measured by ECM production.[13] These findings suggest that hydrogels for MSC-based cartilage TE must preserve viability while still promoting chondrogenic conversion and functional maturation.

In our previous studies showing differences in construct mechanical properties between CHs and MSCs, it was not clear whether the lower properties achieved by MSCs were due to a fundamental limitation in chondrogenesis, or whether this functional maturation could be influenced by the 3D environment (i.e., hydrogel) in which the cells were placed. To further address this question, this study examined the potential of bovine MSCs to undergo chondrogenesis in 3D culture in three distinct hydrogels. We employed agarose (AG, as used previously)[24] and two hydrogels based on natural materials. The first, a commercially available self-assembling peptide gel (Puramatrix, Pu), possesses favorable properties for the culture of numerous cell types and supports CH-mediated ECM deposition.[32,33] More recently, we and others have demonstrated that equine[34] and human[35] MSCs undergo chondrogenesis in this hydrogel. While not providing specific receptor-mediated interactions (e.g., RGD signaling cascades are not activated), the gel does appear to promote cell adhesion and neurite extension[36] and may further be susceptible to proteolytic breakdown. The second biopolymer used was a photocrosslinked hyaluronan (HA)–based hydrogel. This gel supports ECM deposition by articular and auricular CHs, both *in vitro* and *in vivo*.[37–39] HA expression is regulated during limb bud formation and mesenchymal cell condensation, and is a primary structural component of adult cartilage ECM.[40,41] CHs interact with HA in the pericellular environment via CD44 receptors located on the cell surface[42,43] and actively endocytose HA fragments.[44] Thus, relative to the inert, noninteractive and nondegradable AG hydrogel used in our previous studies, these two hydrogels provide an interactive and degradable, biologically relevant interface that might modulate MSC chondrogenesis and construct maturation.

To carry out this study, bovine CHs and MSCs were isolated from the same group of donors and seeded in AG, Pu, and HA hydrogels. Constructs were cultured for 8 weeks with biweekly analysis of construct physical properties, MSC viability, ECM content, and mechanical properties. To further investigate the relationship between deposited ECM and mechanical outcomes, we performed correlation analysis of the emerging structure (composition) and function (mechanical properties) of constructs formed from each cell type in each hydrogel.

Materials and Methods

Cell isolation and expansion

Bovine CHs and MSCs were isolated from juvenile bovine joints within 36 h of slaughter (Research 87, Boylston, MA). Articular CHs were enzymatically isolated from carpometacarpal articular cartilage as previously described.[45] CHs were seeded in hydrogels immediately upon isolation. Bone marrow–derived MSCs were isolated from the underlying trabecular region of the carpal bone as described by Mauck *et al*.[24] To obtain a sufficient number of MSCs, cells were expanded in Dulbecco's modified Eagle's medium (DMEM) supplemented with 10% fetal bovine serum (FBS; Gibco, Invitrogen, Carlsbad, CA) and 1× penicillin–streptomycin–fungizone (PSF) through passage 2 or 3. Both CHs and MSCs were seeded at a density of 20 million cells/mL in AG, methacrylated HA (MeHA), and self-assembling peptide hydrogels. Two complete studies were performed with cells from a minimum of three donor animals pooled for each experiment. Similar trends were observed in each replicate, with data from one study presented in this manuscript.

Cell seeding in hydrogels

To produce cell-laden AG gels, type VII AG (Sigma Chemicals, St. Louis, MO) was dissolved in phosphate-buffered saline (PBS) at a concentration of 4% w/v, autoclaved, and cooled to 49°C. AG was combined 1:1 with a cell suspension (40 million/mL) of either CHs or MSCs in DMEM to provide a seeding density of 20 million cells/mL in a 2% w/v AG hydrogel. The cell–hydrogel suspension was cast between two glass plates separated by 2.25-mm-thick spacers and gelled at 25°C for 20 min. Cylindrical constructs were removed from gel slabs using a sterile 5-mm-diameter biopsy punch (Miltex, York, PA).

Photocrosslinkable MeHA solutions were produced as previously described.[38] Briefly, 65 kDa HA (Lifecore, Chaska, MN) was methacrylated by reaction with methacrylic anhydride (Sigma Chemicals) at pH 8.0 for 24 h, dialyzed in distilled water against a 5 kDa MW cutoff, lyophilized,

and stored at −20°C.[38,39,46] MeHA was dissolved to 2% w/v in PBS supplemented with 0.05% w/v of the photoinitiator I2959 (2-methyl-1-[4-(hydroxyethoxy)phenyl]-2-methyl-1-propanone; Ciba-Geigy, Tarrytown, NY). To produce cell-laden gels, cells were resuspended in the MeHA macromer solution (20 million cells/mL) and the suspension cast between glass plates as above. Polymerization was achieved with UV exposure through the glass plates for 10 min using a 365 nm Blak-Ray UV lamp (Model #UVL-56; San Gabriel, CA). Cylindrical constructs were cored from the resulting slab with a 5-mm-diameter biopsy punch.

The self-assembling peptide hydrogel solution was purchased as Pu ($(REDA)_4$, 1%w/v; BD Bioscience, San Jose, CA). CHs (isolated immediately) or MSCs (after trypsinization) were washed twice in a sterile 10% w/v sucrose solution to remove residual culture medium. Cell pellets were resuspended at 40 million cells/mL in 10% sucrose solution and mixed well with an equal volume of 1% w/v Pu solution to produce a final concentration of cell-seeded 0.5% Pu (w/v). A sterile neoprene rubber mold with cylindrical cavities (5 mm diameter; 2.25 mm thickness) was placed on the bottom of a 100 mm culture dish. Cell/Pu solution was pipetted into the void spaces, and sterile filter paper (prewetted with DMEM) was placed over the mold. The filter paper served as both a source and a path for diffusion of ions from the culture medium to initiate self-assembling peptide polymerization. A glass plate was then added to sandwich the filter paper to the mold to ensure an even construct surface. Sufficient medium to cover the molds was added, and constructs were allowed to polymerize for 30 min. The molding apparatus was then carefully disassembled, and constructs were removed to non-tissue culture–treated six-well plates.

Construct culture and analysis

Constructs were cultured (1 mL/construct) in TGF-β3 (10 ng/mL; R&D Systems, Minneapolis, MN) supplemented, chemically defined chondrogenic medium consisting of high-glucose DMEM with 1× PSF, 0.1 μM dexamethasone, 50 μg/mL ascorbate 2-phosphate, 40 μg/mL l-proline, 100 μg/mL sodium pyruvate, and ITS + (6.25 μg/mL insulin, 6.25 μg/mL transferrin, 6.25 ng/mL selenous acid, 1.25 mg/mL bovine serum albumin, and 5.35 μg/mL linoleic acid) in non-tissue culture–treated six-well plates. Media were changed twice weekly. Encapsulated cell viability was visualized with the Live/Dead assay (Invitrogen, Eugene, OR). Samples for Live/Dead were cross-sectioned with a sterile scalpel and rinsed twice in sterile PBS before being incubated for 20 min (at 20°C) in a PBS solution containing 2 μM Calcein AM and 4 μM ethidium homodimer-1. Stained construct cross sections were imaged using an inverted fluorescence microscope (Nikon T30; Nikon Instruments, Melville, NY).

Mechanical testing

Mechanical testing in unconfined compression was carried out biweekly to determine equilibrium and dynamic properties as described by Mauck *et al*.[24] On the day of testing, sample dimensions were measured with a digital caliper. Creep tests were then performed in a PBS bath between two impermeable platens with a 2 g load applied and displacement monitored until equilibrium (~300 s). Subsequently, stress relaxation tests were performed by applying a single compressive deformation to 10% strain (at 0.05%/s) followed by 20 min of relaxation to equilibrium. The equilibrium modulus was calculated from the equilibrium stress and strain values based on the measured construct dimensions. Dynamic testing was then carried out via the application of a sinusoidal deformation of 1% applied at 1.0, 0.5, and 0.1 Hz for 10 cycles. The dynamic modulus for each sample was calculated from the slope of the dynamic stress–strain curve as in Park *et al*.[47]

Biochemical analyses

After compression testing, construct wet weights were recorded, and samples were digested in papain for analysis of DNA, sulfated glycosaminoglycan (s-GAG), and collagen content.[24] DNA content (per construct) was determined using the dsDNA Picogreen Assay (Molecular Probes, Eugene, OR) with λDNA as a standard. s-GAG content (total and percent wet weight) was determined using the 1,9-dimethylmethylene blue dye binding assay with chondroitin-6 sulfate as a standard.[48] Digested aliquots were also hydrolyzed for 16 h in 12 N HCl at 110°C, and the orthohydroxyproline (OHP) content was quantified via colorimetric reaction with chloramine T and diaminobenzaldehyde, against an OHP standard curve.[49] Collagen content was extrapolated from OHP using a 1:10 ratio of OHP:collagen.[50]

Histology

Samples from each hydrogel at each time point were fixed in 4% paraformaldehyde, infiltrated with Citrisolv, and embedded in paraffin blocks. Sections (8 μm) were mounted on glass slides and stained for proteoglycan using Alcian blue (pH 1.0) and for collagen via Picrosirius Red as described by Mauck *et al*.[45]

Statistical analyses

Statistical analysis was performed using Systat (v10.2; San Jose, CA). A three-way ANOVA analysis was carried out, with cell type, time in culture, and hydrogel type as independent factors. Dependent variables were wet weight, thickness, diameter, Young's modulus, dynamic modulus, [GAG], [collagen], and DNA content. When significant effects ($p < 0.05$) were observed, Fisher's LSD *post hoc* analysis was used to compare between groups. All values are reported as the mean ± SD. For correlation analyses, GraphPad Prism (San Diego, CA) was used to fit data and determine goodness of fit, and *t*-tests were used to compare correlation slopes between conditions.

Results

3D culture: cell shape, viability, and construct dimensions

Upon encapsulation, CHs and MSCs took on a rounded shape in each hydrogel. In AG, both cell types remained rounded throughout the culture duration, and occasional small clusters could be observed indicative of cell division (Fig. 1). In the photocrosslinked MeHA gels most cells remained rounded, while a minor fraction of both cell populations developed small protrusions. In Pu gels, CHs and MSCs showed both round shape and pronounced filopodial

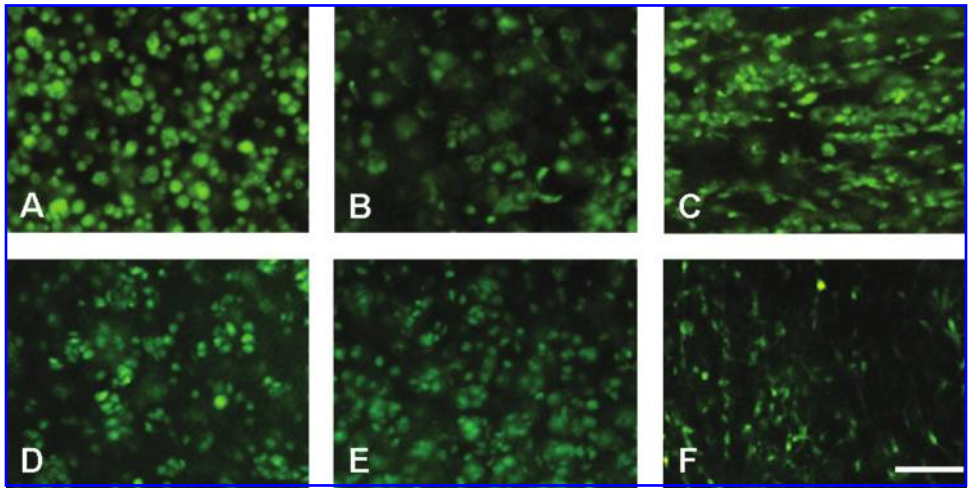

FIG. 1. Calcein AM staining of live cells in construct cross sections on day 42 for CHs (**A–C**) and MSCs (**D–F**) in AG (left), MeHA (middle), and Pu (right) hydrogels. Magnification, 40×; scale bar, 50 μm. Color images available online at www.liebertonline.com/ten.

projections throughout the gel, with this finding more pronounced in MSC cultures. Viability was high for each cell type in all gels, with Live/Dead staining showing no obvious differences between AG, MeHA, and Pu hydrogels on either day 14 or 42 (Fig. 1).

While viability was similar, differences in dimensional characteristics were observed in the three cell-seeded hydrogels. These data are summarized in Table 1. For all constructs, marked increases in wet weight were observed between days 14 and 56 ($p < 0.005$). Increased wet weight correlated with increases in s-GAG and collagen deposition within the construct (increasing its density) as well as changes in construct diameter and thickness. Of significant note, Pu hydrogels seeded with CHs and MSCs decreased in volume over the initial 2 weeks of culture, with the most marked changes in MSC-laden construct diameters (>40% reduction for Pu-MSC, $p < 0.001$ vs. day 0). This decrease in diameter slowly reversed with time, but remained <30% of the starting diameter on day 56. These changes in size translated to changes in Pu wet weight, with both CH- and MSC-laden Pu gels significantly lower than all other gels at day 56 ($p < 0.001$). Conversely, MeHA gels increased in size with culture duration, particularly in the axial direction, increasing by ~25% and ~37% in thickness by day 56 for CH- and MSC-seeded conditions, respectively ($p < 0.001$). AG hydrogels underwent only minor changes in dimensions throughout the culture period with either cell type.

Biochemical composition and histological analysis

Biochemical and histological analysis of constructs was carried out on a biweekly basis for each gel type and each cell type. In general, increasing time led to more matrix accumulation in each gel for each cell type as shown by histology and quantification of deposited ECM. For all CH-laden gels, DNA content increased two to three times over the 8-week culture period ($p < 0.001$, Fig. 2A). On day 56, there was no significant difference between the total DNA content of each hydrogel construct. In MSC-laden constructs, little change in DNA content was observed over the 8-week

Table 1. Construct Dimensions and Biochemical Content

	2% AG		*2% MeHA*		*0.5% Pu*	
CHs	*2 weeks*	*8 weeks*	*2 weeks*	*8 weeks*	*2 weeks*	*8 weeks*
Wet weight (mg)	43.7 ± 1.5^a	57.5 ± 2.7^b	46.5 ± 2.6^a	66.2 ± 4.6^b	24.2 ± 3.6^a	35.0 ± 3.0^b
s-GAG (μg)	553.8 ± 44.2^a	1868.1 ± 232.3^b	173.5 ± 9.6^a	647.1 ± 70.1^b	77.7 ± 33.6	717.1 ± 178.3^b
Collagen (μg)	194.6 ± 18.9^a	1200.4 ± 121.5^b	36.2 ± 10.0	276.3 ± 33.8^b	24.7 ± 10.3	530.9 ± 128.9^b
Thickness (% change)	3.9 ± 1.9	12.0 ± 1.7^b	11.4 ± 2.1^a	25.1 ± 7.7^b	-26.8 ± 6.9^a	-3.5 ± 9.3^c
Diameter (% change)	-0.8 ± 0.8	6.2 ± 1.1^b	-5.2 ± 0.1^a	3.8 ± 0.2^c	-15.4 ± 0.5^a	-11.2 ± 6.1^b
MSCs	*2 weeks*	*8 weeks*	*2 weeks*	*8 weeks*	*2 weeks*	*8 weeks*
Wet weight (mg)	46.6 ± 0.9^a	58.5 ± 3.9^b	65.2 ± 0.6^a	87.3 ± 1.0^b	15.9 ± 0.9^a	21.0 ± 2.6^b
s-GAG (μg)	702.2 ± 86.1^a	1455.4 ± 181.2^b	633.2 ± 32.4^a	1602.7 ± 91.4^b	306.3 ± 21.4^a	819.2 ± 135.1^b
Collagen (μg)	211.1 ± 20.9^a	718.3 ± 192.4^b	204.9 ± 19.2^a	738.1 ± 170.7^b	134.1 ± 20.9^a	388.1 ± 72.5^b
Thickness (% change)	1.7 ± 1.2	13.4 ± 2.5^b	23.3 ± 3.0^a	37.1 ± 2.1^b	-3.0 ± 8.8	2.1 ± 5.4
Diameter (% change)	0.7 ± 1.1	7.9 ± 4.6^b	2.3 ± 1.3	16.1 ± 2.1^b	-42.2 ± 1.62^a	-30.1 ± 3.6^b

Time-dependent changes in construct dimensions and biochemical content. Data represents the mean ± SD of three to four samples for each group at each time point.

[a] $p < 0.05$ versus day 0.

[b] $p < 0.05$ versus day 0 and day 14.

[c] $p < 0.05$ from day 14.

CH, chondrocytes; MSC, mesenchymal stem cells.

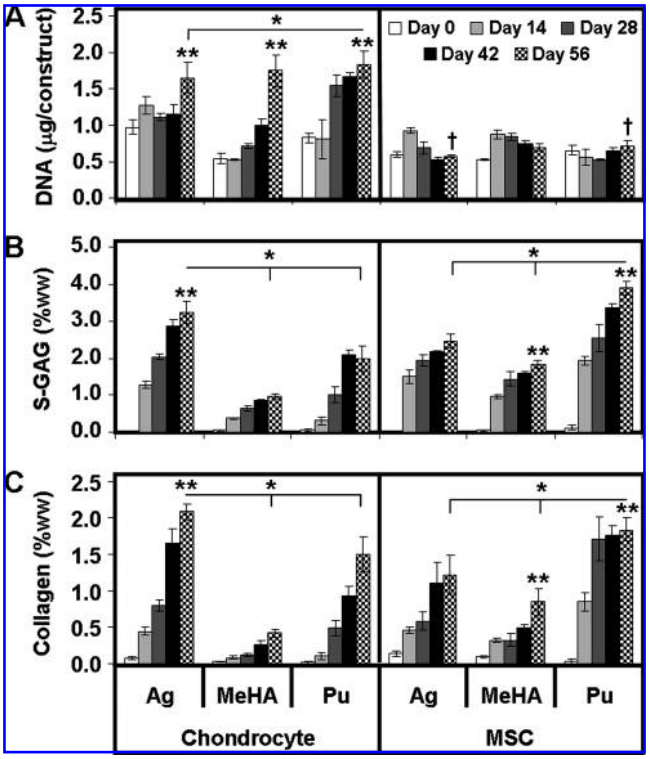

FIG. 2. Biochemical content of CH- and MSC-seeded constructs as a function of time over an 8-week culture period. (**A**) DNA content, (**B**) s-GAG as a percentage of the wet weight (ww), and (**C**) collagen as a percentage of the wet weight. Data represent the mean ± SD of three to four samples from one of two replicate studies. *$p < 0.05$ for day 56 comparisons between hydrogels within cell type. **Greater value ($p < 0.05$) for comparisons on day 56 within hydrogel between cell types. †No significant increase from day 0 ($p > 0.05$).

time course. MeHA–MSC and Pu–MSC constructs contained ~20% more DNA/construct than AG–MSC constructs on day 56 (Fig. 2A; MeHA, $p = 0.08$; Pu, $p = 0.06$, vs. AG).

Overall ANOVA results showed that s-GAG deposition in each hydrogel was dependent on time in culture ($p < 0.001$), hydrogel type ($p < 0.001$), and cell type ($p < 0.001$). For CHs and MSCs, significant increases in s-GAG content were observed in each gel (Fig. 2B, $p < 0.001$). On day 56, AG–CH gels contained 1.5–3-fold greater s-GAG per wet weight (ww) than MeHA–CH and Pu–CH gels did. AG–CH gels attained ~3.2%ww s-GAG and were significantly greater ($p < 0.001$) than both Pu–CH (~2%) and MeHA–CH (~1%) gels (Fig. 2B). Conversely, AG–MSC and MeHA–MSC hydrogels contained similar amounts of s-GAG on a per wet weight basis, while Pu–MSC gels were nearly two times greater. Pu–MSC gels contained ~3.9% wet weight s-GAG, which was greater ($p < 0.001$) than both AG–MSC (~2.5%) and MeHA–MSC (~1.8%) gels (Fig. 2B). Indeed, this value was higher than the highest value achieved for CH-seeded gels (AG–CH group, $p < 0.001$). Most interestingly, this was not the result of increased s-GAG production in Pu–MSC gels, but rather was the result of the reduction in volume observed; on a per construct basis, AG–MSC and MeHA–MSC gels contained 1500–1600 µg of s-GAG compared to ~800 µg for Pu–MSC gels (Table 1).

Similar to s-GAG results, collagen content was dependent on time in culture ($p < 0.001$), gel type ($p < 0.001$), and cell type ($p < 0.001$). Collagen content as a function of wet weight was 1.4–5-fold greater in AG–CH than in MeHA–CH and Pu–CH constructs. AG–CH gels contained ~2.1%ww collagen, a higher level than in Pu–CH (~1.5%) and MeHA–CH (~0.4%, $p < 0.02$, Fig. 2C) constructs. In terms of collagen content per construct, AG–CH contained twofold greater collagen than Pu–CH and fourfold greater collagen than MeHA–CH constructs ($p < 0.001$, Table 1). Conversely, Pu–MSC gels contained the highest collagen content (1.8%), levels greater than for AG–MSC (1.2%, $p < 0.001$), and both greater than MeHA–MSC (0.8%, $p < 0.001$) constructs. For these MSC cultures, the highest collagen density observed (in the Pu–MSC group) was only slightly lower than that found for the best CH-laden hydrogel group (AG–CH, $p < 0.02$). As with s-GAG content, the apparent improvement in collagen content in Pu–MSC constructs was more a function of dimensional changes, with approximately twofold less total collagen in these constructs compared to either AG or MeHA on a per construct basis (Table 1, $p < 0.001$).

Histological staining of constructs produced findings consistent with gross biochemical measures. Alcian blue staining of s-GAG deposition in CH- and MSC-seeded constructs correlated well with biochemical measures (Fig. 3A–F). Noticeably weaker s-GAG deposition was observed in MeHA–CH sections relative to all other groups. Picrosirius red staining of collagen elicited similar results; AG–CH and Pu–CH constructs stained much more intensely for collagen than MeHA–CH constructs did. More collagen was observed in MeHA–MSC constructs, though staining remained less intense and less evenly distributed than in either AG–MSC or Pu–MSC constructs (Fig. 3G–L).

Mechanical properties

The equilibrium (E_Y) and dynamic (G^*) compressive mechanical properties of cell-seeded constructs were evaluated over the 8-week time course (Fig. 4). Overall, time, gel type, and cell type were significant factors in both mechanical measures ($p < 0.05$). The equilibrium modulus (E_Y) of CH-seeded constructs increased with time relative to their starting values ($p < 0.001$ on day 28 for AG–CH, and $p < 0.05$ on day 42 for Pu–CH; for MeHA–CH, $p = 0.343$ on day 56), though Pu constructs were too soft for mechanical testing until day 28. On day 56, E_Y of AG–CH constructs reached ~170 kPa, a value fivefold to sevenfold ($p < 0.001$) greater than that of either MeHA–CH or Pu–CH constructs. Similar findings were noted with regard to G^*, though the differences between groups were accentuated. On day 56, AG–CH constructs reached a G^* of ~1 MPa, a level 20- and 10-fold greater ($p < 0.001$) than MeHA–CH and Pu–CH constructs, respectively.

A different functional maturation process was noted for MSC-seeded constructs, with increases in equilibrium properties comparable between each hydrogel. Each hydrogel seeded with MSCs increased in E_Y as a function of time in culture ($p < 0.005$ vs. day 0 on day 14 for AG–MSC, day 42 for MeHA–MSC, and day 28 for Pu–MSC). The E_Y of AG–MSC constructs on day 56 was ~100 kPa, compared to ~60 kPa for MeHA–MSC gels and ~80 kPa for Pu–MSC gels. At this time point, E_Y of MSC-seeded constructs were

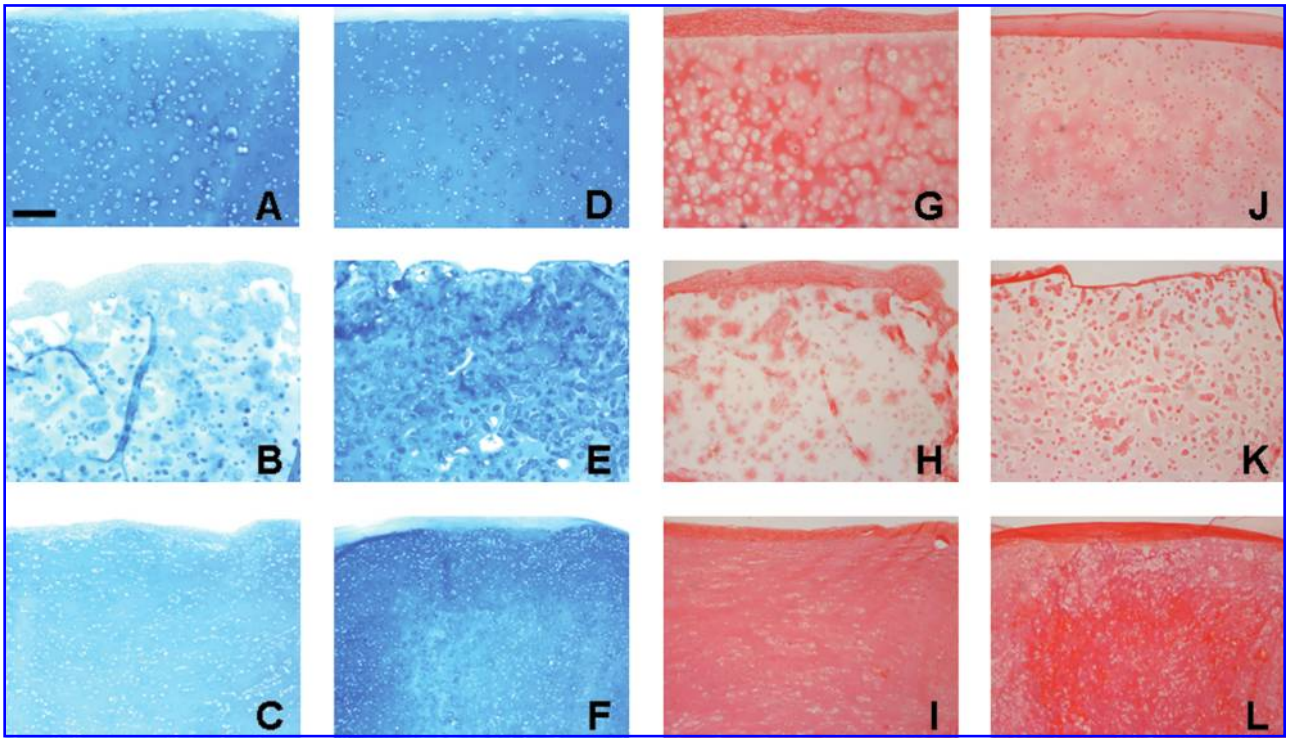

FIG. 3. Histological analysis of CH- and MSC-seeded constructs on day 56. Alcian blue staining of deposited PGs for CH-seeded (**A–C**) and MSC-seeded (**D–F**) AG (top), MeHA (middle), and Pu (bottom) hydrogels. Picrosirius red staining of deposited collagen for CH-seeded (**G–I**) and MSC-seeded (**J–L**) AG (top), HA (middle), and Pu (bottom) hydrogels. Magnification, 100×; scale bar, 200 μm. Color images available online at www.liebertonline.com/ten.

similar to one another, with significant difference only found between AG–MSC and MeHA–MSC ($p < 0.01$). Similarly, the G^* of AG–MSC constructs increased with time ($p < 0.001$ vs. day 0), reaching a value of ~0.15 MPa on day 56. G^* values for MeHA–MSC and Pu–MSC increased with time as well, reaching 0.04 MPa and 0.12 MPa, respectively. At this time point, G^* for AG–MSC and Pu–MSC gels were not different from one another ($p = 0.37$), while the G^* of the MeHA–MSC group was significantly lower than both ($p < 0.05$). For both E_Y and G^*, the highest values achieved for MSC-laden

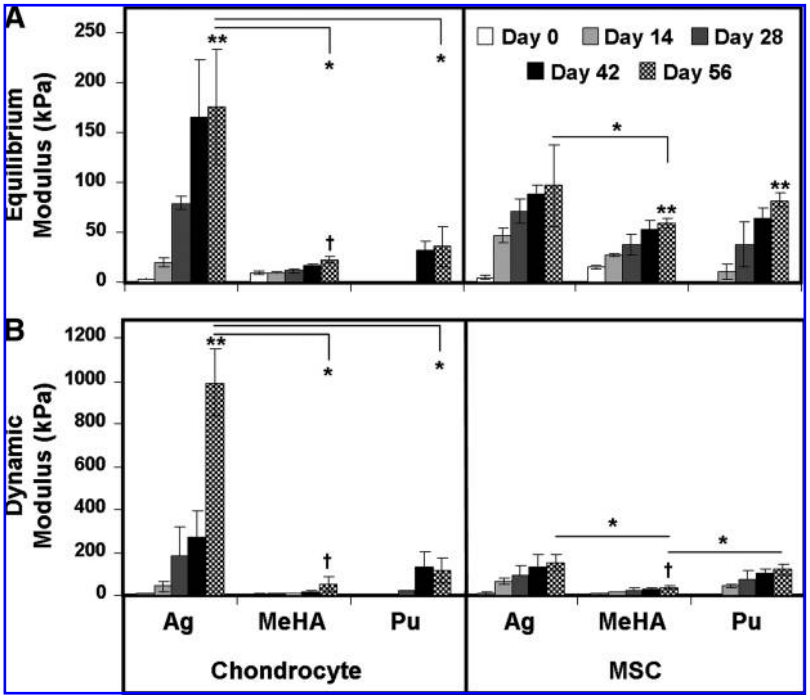

FIG. 4. (**A**) Equilibrium modulus, E_Y, and (**B**) dynamic modulus, G^*, of AG, MeHA, and Pu hydrogels seeded with CHs or MSCs measured bi-weekly over a 56-day culture period. Data represent the mean ± SD of three to four samples from one of two replicate studies. *$p < 0.05$ for day 56 comparisons between hydrogels within cell type. **Greater value ($p < 0.05$) for comparisons on day 56 within hydrogel between cell types. †No significant increase from day 0 ($p > 0.05$).

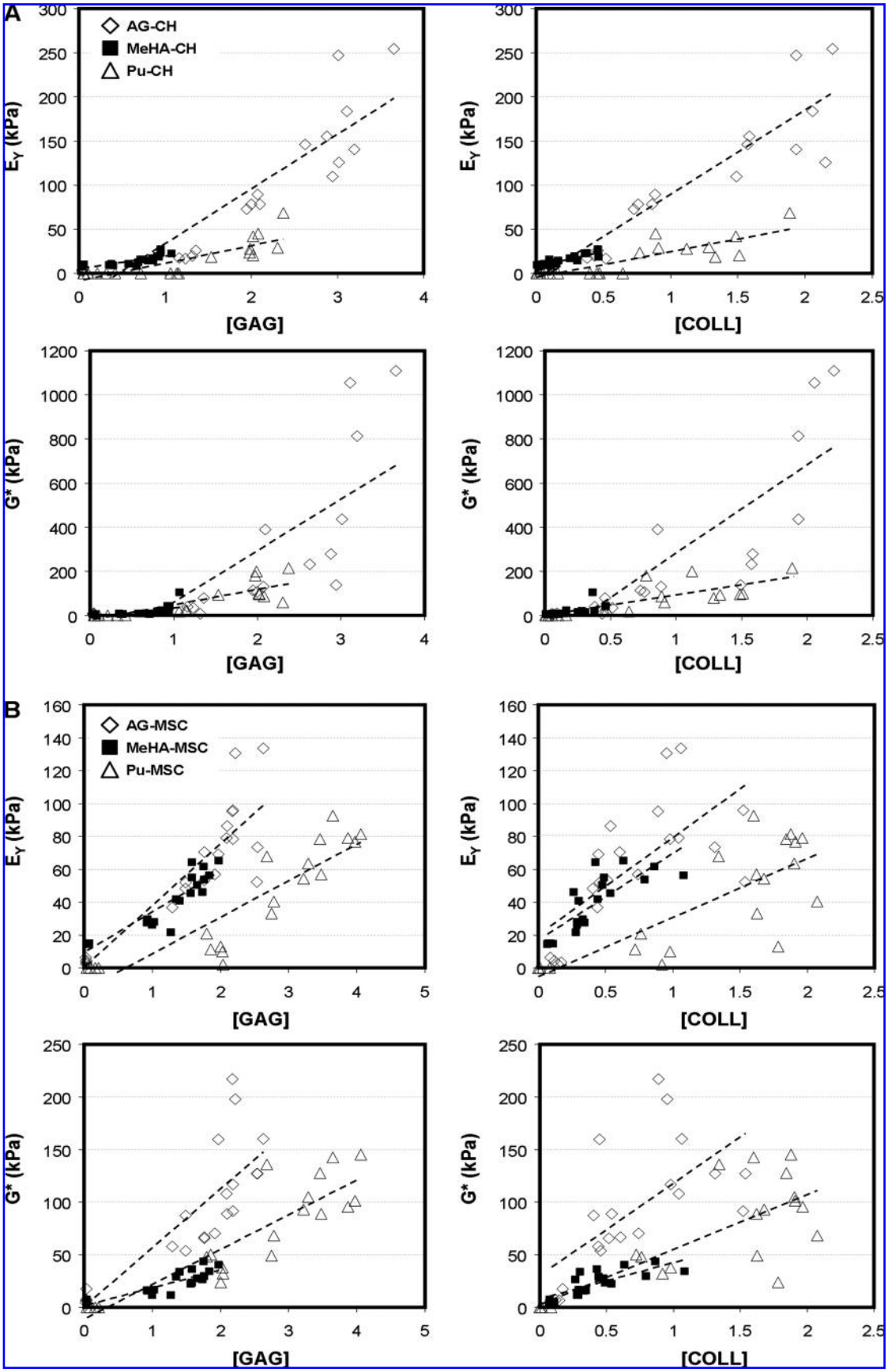

FIG. 5. Correlation plots relating measured mechanical properties to biochemical constituents. (**A**) Plots for CH-seeded hydrogels. (**B**) Plots for MSC-seeded hydrogels. Dashed line shows linear curve fit for each gel type.

Table 2. Structure–Function Correlations

		CHs				MSCs				
Gel	*Comparison*	*Slope*	R^2	p	*Versus AG*	*Slope*	R^2	p	*Versus AG*	*Versus CHs*
Agarose	E_Y vs. [GAG]	62.9	0.800	<0.0001		37.6	0.752	<0.0001		[a]
	E_Y vs. [COLL]	96.9	0.857	<0.0001		59.1	0.478	0.0004		NS
	G^* vs. [GAG]	233.9	0.490	0.0006		56.1	0.658	<0.0001		[b]
	G^* vs. [COLL]	405.8	0.694	<0.0001		87.9	0.414	0.0011		[a]
MeHA	E_Y vs. [GAG]	13.9	0.654	<0.0001	[b]	24.7	0.925	<0.0001	[c]	NS
	E_Y vs. [COLL]	34.2	0.800	<0.0001	[b]	52.8	0.645	<0.0001	NS	[c]
	G^* vs. [GAG]	44.6	0.392	0.0021	[a]	17.0	0.753	<0.0001	[b]	[b]
	G^* vs. [COLL]	106.9	0.455	0.0008	[a]	34.6	0.584	<0.0001	[b]	[b]
Puramatrix	E_Y vs. [GAG]	20.0	0.696	<0.0001	[b]	22.2	0.803	<0.0001	[c]	NS
	E_Y vs. [COLL]	28.9	0.72	<0.0001	[b]	35.0	0.630	<0.0001	[c]	NS
	G^* vs. [GAG]	69.4	0.668	<0.0001	[b]	33.0	0.793	<0.0001	[b]	[b]
	G^* vs. [COLL]	95.2	0.642	<0.0001	[b]	52.2	0.595	<0.0001	[c]	[a]

Correlation of mechanical properties and biochemical content in CH- and MSC-seeded constructs. Correlation coefficients relating measured mechanical properties (E_Y and G^*) with concentration of s-GAG and collagen for CH- and MSC-seeded constructs.
[a] $p < 0.05$.
[b] $p < 0.001$.
[c] $p < 0.01$.
NS, no significant difference.

hydrogels on day 56 were lower than that achieved for the AG–CH group ($p < 0.001$ and $p < 0.001$, respectively).

Structure–function correlation analysis

To better elucidate the relationships between new matrix deposition and functional maturation, correlation analyses were performed between the level of a given biochemical constituent and the resulting construct mechanical properties. Specifically, E_Y and G^* were correlated to the concentration (as a percentage of wet weight) of s-GAG and collagen in each construct for each cell type and each hydrogel formulation. The results of these correlations are shown in Figure 5, and the slopes and correlation coefficients are provided in Table 2. For each comparison, a significant linear fit was achieved ($p < 0.005$), with R^2 values ranging from 0.392 to 0.925. For CH-seeded constructs, the slope of the correlations was uniformly higher for AG–CH gels than for either the MeHA–CH and Pu–CH gels ($p < 0.05$). For example, the slope of E_Y vs. [GAG] for AG–CH gels was 62.9 kPa/%ww, and was significantly higher than for MeHA (13.9 kPa/%ww) and Pu (20.0 kPa/%ww) constructs. For MSC-laden constructs, modest differences were observed between gel types (all lower, $p < 0.01$ compared to AG except for MeHA E_Y vs. [COLL], $p = 0.08$). For the same comparison as above on MSC-laden constructs (E_Y vs. [GAG]), correlation slopes were 37.6, 24.7, and 22.2 kPa/%ww for AG–MSC, MeHA–MSC, and Pu–MSC, respectively. Finally, comparing the same correlation slopes across cell types allows one to draw conclusions regarding the ability of MSCs to produce functional matrix relative to a CH control. For all AG–MSC groups except E_Y vs. [COLL] ($p = 0.367$), correlation slopes were lower in AG–MSC than in AG–CH samples ($p < 0.05$). For MeHA–MSC and Pu–MSC constructs, the correlation slopes of E_Y were generally higher than those achieved in the corresponding CH group. Conversely, the G^* slopes in MeHA–MSC and Pu–MSC were lower than their CH counterparts ($p < 0.005$). In either case, for both E_Y and G^*, the correlation slopes for the MSC-laden constructs remained well below that achieved in AG–CH constructs ($p < 0.05$).

Discussion

The goal of this study was to evaluate the functional formation of cartilage tissue in three distinct MSC-laden hydrogels, and to compare these findings to those produced by fully differentiated CHs maintained in the same culture environment. The motivation for this study was based on our previous finding that in AG hydrogels, MSCs underwent chondrogenesis, but formed cartilage-specific ECM of lower quantity and quality than constructs formed with donor-matched fully differentiated CHs cultured under the same conditions. Given the growing body of evidence supporting biomaterial-dependent stem cell differentiation, we hypothesized that cell–hydrogel interactions would modulate the rate and extent of functional chondrogenesis. Results of this study show that, surprisingly, the external hydrogel environment plays a more significant role in CH-mediated than in MSC-mediated matrix deposition and functional maturation. Articular CHs formed the most mechanically robust ECM in AG hydrogels, followed by Pu and then MeHA gels. Conversely, MSC-laden hydrogels showed similar results across gel types, with marked increases in mechanical properties in each gel. However, in each case, the maximum compressive properties achieved in MSC-laden constructs remained lower than that achieved by fully differentiated CHs in AG gels. These findings are consistent with our previous observations,[24,29] and further support the notion that existing methodologies for effecting MSC chondrogenesis in 3D culture have not yet been optimized to produce cells possessing functional matrix forming capacity on par with that of a fully differentiated CHs.

Several important observations were made regarding differential biomaterial effects on construct formation with either CHs or MSCs. Notably, changes in construct size were pronounced in the differing hydrogels. We have previously

reported only minor changes in construct diameter and thickness in AG hydrogels seeded with CHs or MSCs.[24] Findings in AG in this study were consistent with that observation, and further showed pronounced increases in volume in cell-seeded MeHA gels (particularly in the axial direction), and a marked reduction in volume in Pu-based constructs, particularly when seeded with MSCs. These changes in Pu construct volume are consistent with recent work by Kisiday *et al*., who reported decreases in construct diameter in bone marrow and adipose-derived MSC-seeded constructs seeded in ~0.4% $(KLDL)_3$ self-assembling peptide gels.[34] This change in construct size may limit clinical application to constructs that have been prematured *in vitro*, punched to size, and then implanted into defined cartilage defects. More generally, this contraction suggests that cell-mediated traction is occurring, as has similarly been reported when constructs are formed using gelatin sponges.[27] Indeed, both CHs and MSCs were elongated with numerous cell protrusions in the Pu constructs. One consequence of this volume reduction in Pu-based gels was to increase the effective concentration of s-GAG and collagen within the constructs, though the total amount per construct was lower than that produced by CHs. The decreased volume resulted in Pu-based constructs reaching levels of s-GAG and collagen concentrations (on a percentage wet weight basis) comparable to that observed for CHs seeded in AG gels. Notably, DNA content on day 56 in each MSC-seeded hydrogel was comparable, suggesting that the production levels, on a per cell basis, were lower in Pu hydrogels. Regardless of this concentration effect, Pu–MSC mechanical properties did not match those of AG–CH constructs.

Another observation in this study was that articular CHs in MeHA did not readily form functional matrix. This finding is consistent with our previous studies comparing auricular and articular CHs in this hydrogel,[46] wherein auricular CHs produced a considerably more robust ECM than articular CHs. In this previous work, constructs were cultured both *in vivo* (subcutaneously) and *in vitro* in a serum-containing medium. Here we show that *in vitro* culture in a chemically defined pro-chondrogenic media formulation does not restore functional capacity to articular CHs in this gel. This finding of lower ECM formation was not a function of cell death due to UV or photoinitiator exposure as DNA content increased similarly for CHs in this gel as in the other two culture systems assayed. This suggests that the MeHA gel, in its present formulation, may not be optimized for articular-derived cells. While it is not yet clear whether matrix was made in lower quantities, or made in the same quantity and lost from the gel during culture, it is clear that these CH-seeded MeHA constructs will require further modification to optimize their growth. More generally, these findings suggest that CHs are more sensitive to the gel environment than MSCs (which performed much better in this MeHA formulation). This was a surprising result, given that articular CHs are largely anchorage independent (as they can live well in cell aggregates[51]), while MSCs require a defined extracellular niche. This finding suggests that MeHA gel properties may be optimized to improve construct maturation. For example, we have recently shown that the starting concentration of the MeHA solution (and so the starting mechanical properties of the hydrogel) alters the final mechanical properties of MSC-seeded constructs after 9 weeks of culture,[52] and that a new hydrolytically degradable MeHA formulation promotes more rapid distribution of formed ECM components.[53] By altering the biomaterial environment in these covalently crosslinked HA assemblies, an optimal environment for MSC chondrogenesis that is both permissive and pro-chondrogenic may be achieved.

To better understand how matrix deposition related to functional maturation in these constructs, we carried out a single-factor correlation analysis for each hydrogel and cell type. Similar analyses have previously been performed for CHs and MSCs seeded in degradable meshes and hydrogels.[27,50,54] The results of this analysis show how, for a given amount of ECM deposition, mechanical outcomes vary between conditions. In AG–CH constructs, we found a strong positive correlation between s-GAG and E_Y, and show that for MeHA and Pu constructs, the correlation slopes were smaller. This indicates that not only do AG–CH constructs make more s-GAG, but also the functional consequence of a given amount of s-GAG is greater in this hydrogel. While s-GAG levels were generally lower in MeHA and Pu gels than AG, collagen concentration in Pu and AG were comparable. However, the correlation slope for this ECM component was lower for the Pu samples, indicating inferior matrix assembly. For the MSC-laden cultures, a different trend was observed. For these cells, in each gel type, similar correlation slopes were achieved. This suggests that between gels, MSCs assemble functional matrix in a similar fashion, though the slopes of these correlations were lower than that found for the same comparison in AG–CH hydrogels. This finding further supports the notion that MSCs elaborate ECM that is inferior to that produced by fully differentiated CHs. While not identified in the current study, we hypothesize that there exists critical structural ECM components whose expression and deposition is not yet optimized in MSC cultures. These factors must be identified and exploited to allow MSC-based constructs to achieve properties similar to that produced by AG–CH constructs for functional cartilage TE applications.

While robust growth was observed in MSC-seeded constructs, biochemical content and mechanical properties did not yet meet that of the native tissue. For example, while s-GAG content reached 3–4%ww for AG–MSC and Pu–MSC cultures (near physiologic levels), the highest collagen content achieved was ~2%ww, less than 20% of the native tissue. It should be noted that this low collagen content was found in both MSC- and CH-based cultures, and is a persistent limitation in engineered cartilage.[55] Moreover, we did not specifically measure type I versus type II collagen ratios, which may well have differed in the differing hydrogels, particularly those that showed considerable contraction. Further, while MSC-laden cultures reached equilibrium compressive properties that were ~25% that of bovine cartilage (and ~50% that of CH cultures), the dynamic modulus of MSC-based constructs only reached ~0.2 MPa (as compared to 1 MPa for CH-based constructs). The dynamic modulus is a critical mechanical feature of the native tissue, and consequently these values must be further optimized to enable *in vivo* function. Additional quantification of other mechanical features of these constructs, such as the hydraulic permeability and tensile properties, would also be useful in understanding the key differences among cell types and 3D culture conditions.

The results of this study demonstrate biomaterial-dependent functional cartilage tissue formation. In particular, MSC-seeded constructs increased in mechanical properties in each hydrogel, with the most robust maturation reaching 100 kPa, ¼ the value of native bovine tissue. Continuing work is focused on further optimization of gel properties (as detailed above) and culture conditions to improve MSC-based construct maturation. Recent reports have shown that the passive mechanical properties of the material can influence MSC differentiation in 2D cultures.[56] These changes are slightly more difficult to achieve in 3D cultures, as changing the stiffness of the 3D network often requires concomitant changes in permeability, but such studies warrant further consideration. Alternatively, we have shown that dynamic loading can improve CH-based AG construct maturation,[45,57] and that articular CHs in MeHA gels alter matrix gene expression with mechanical loading.[58] Similarly, dynamic loading increased construct properties of CH-seeded Pu hydrogels.[59] We and others have further demonstrated that mechanical loading can modulate MSC chondrogenesis in 3D hydrogel culture.[60–62] These and other optimization strategies offer multiple avenues for improving MSC-based engineered cartilage constructs.

Acknowledgments

This work was supported by grants from the National Institutes of Health [RO3 AR053668 (R.L.M.) and K22 DE-015761 (J.A.B.)]. Additional support was provided through National Science Foundation Graduate Research Fellowships (I.E.E., A.H.H., and C.C.) and an NSF-sponsored REU Summer Undergraduate Research Program (R.T.L.). Further support was provided by the Penn Center for Musculoskeletal Disorders (NIH AR050950).

Disclosure Statement

No competing financial interests exist.

References

1. Ateshian, G.A., and Hung, C.T. Patellofemoral joint biomechanics and tissue engineering. Clin Orthop Relat Res **436,** 81–90, 2005.
2. Mow, V.C., Ratcliffe, A., and Poole, A.R. Cartilage and diarthrodial joints as paradigms for hierarchical materials and structures. Biomaterials **13,** 67–97, 1992.
3. Stockwell, R.A. Biology of cartilage cells. Biological Structure and Function. Cambridge, NY: Cambridge University Press, 1979.
4. Guilak, F., Sah, R.L., and Setton, L.A. Physical regulation of cartilage metabolism. In: Mow, V.C., and Hayes, W.C., eds. Basic Orthopaedic Biomechanics. Philadelphia: Lippincott-Raven 1997, pp. 179–207.
5. Grodzinsky, A.J., Levenston, M.E., Jin, M., and Frank, E.H. Cartilage tissue remodeling in response to mechanical forces. Annu Rev Biomed Eng **2,** 691–713, 2000.
6. Hung, C.T., Mauck, R.L., Wang, C.C., Lima, E.G., and Ateshian, G.A. A paradigm for functional tissue engineering of articular cartilage via applied physiologic deformational loading. Ann Biomed Eng **32,** 35–49, 2004.
7. Kuo, C.K., Li, W.J., Mauck, R.L., and Tuan, R.S. Cartilage tissue engineering: its potential and uses. Curr Opin Rheumatol **18,** 64–73, 2006.
8. Chung, C., and Burdick, J.A. Engineering cartilage tissue. Adv Drug Deliv Rev **60,** 243–262, 2008.
9. Benya, P.D., and Shaffer, J.D. Dedifferentiated chondrocytes reexpress the differentiated collagen phenotype when cultured in agarose gels. Cell **30,** 215–224, 1982.
10. Hauselmann, H.J., Fernandes, R.J., Mok, S.S., Schmid, T.M., Block, J.A., Aydelotte, M.B., Kuettner, K.E., and Thonar, E.J. Phenotypic stability of bovine articular chondrocytes after long-term culture in alginate beads. J Cell Sci **107 (Pt 1),** 17–27, 1994.
11. Buschmann, M.D., Gluzband, Y.A., Grodzinsky, A.J., Kimura, J.H., and Hunziker, E.B. Chondrocytes in agarose culture synthesize a mechanically functional extracellular matrix. J Orthop Res **10,** 745–758, 1992.
12. Burdick, J.A., and Anseth, K.S. Photoencapsulation of osteoblasts in injectable RGD-modified PEG hydrogels for bone tissue engineering. Biomaterials **23,** 4315–4323, 2002.
13. Connelly, J.T., Garcia, A.J., and Levenston, M.E. Inhibition of *in vitro* chondrogenesis in RGD-modified three-dimensional alginate gels. Biomaterials **28,** 1071–1083, 2007.
14. Park, Y., Lutolf, M.P., Hubbell, J.A., Hunziker, E.B., and Wong, M. Bovine primary chondrocyte culture in synthetic matrix metalloproteinase-sensitive poly(ethylene glycol)-based hydrogels as a scaffold for cartilage repair. Tissue Eng **10,** 515–522, 2004.
15. Lutolf, M.P., and Hubbell, J.A. Synthetic biomaterials as instructive extracellular microenvironments for morphogenesis in tissue engineering. Nat Biotechnol **23,** 47–55, 2005.
16. Tallheden, T., Bengtsson, C., Brantsing, C., Sjogren-Jansson, E., Carlsson, L., Peterson, L., Brittberg, M., and Lindahl, A. Proliferation and differentiation potential of chondrocytes from osteoarthritic patients. Arthritis Res Ther **7,** R560–R568, 2005.
17. Tran-Khanh, N., Hoemann, C.D., McKee, M.D., Henderson, J.E., and Buschmann, M.D. Aged bovine chondrocytes display a diminished capacity to produce a collagen-rich, mechanically functional cartilage extracellular matrix. J Orthop Res **23,** 1354–1362, 2005.
18. Schnabel, M., Marlovits, S., Eckhoff, G., Fichtel, I., Gotzen, L., Vecsei, V., and Schlegel, J. Dedifferentiation-associated changes in morphology and gene expression in primary human articular chondrocytes in cell culture. Osteoarthritis Cartilage **10,** 62–70, 2002.
19. Stokes, D.G., Liu, G., Coimbra, I.B., Piera-Velazquez, S., Crowl, R.M., and Jimenez, S.A. Assessment of the gene expression profile of differentiated and dedifferentiated human fetal chondrocytes by microarray analysis. Arthritis Rheum **46,** 404–419, 2002.
20. Pittenger, M.F., Mackay, A.M., Beck, S.C., Jaiswal, R.K., Douglas, R., Mosca, J.D., Moorman, M.A., Simonetti, D.W., Craig, S., and Marshak, D.R. Multilineage potential of adult human mesenchymal stem cells. Science **284,** 143–147, 1999.
21. Prockop, D.J. Marrow stromal cells as stem cells for nonhematopoietic tissues. Science **276,** 71–74, 1997.
22. Johnstone, B., Hering, T.M., Caplan, A.I., Goldberg, V.M., and Yoo, J.U. *In vitro* chondrogenesis of bone marrow-derived mesenchymal progenitor cells. Exp Cell Res **238,** 265–272, 1998.
23. Majumdar, M.K., Wang, E., and Morris, E.A. BMP-2 and BMP-9 promotes chondrogenic differentiation of human multipotential mesenchymal cells and overcomes the inhibitory effect of IL-1. J Cell Physiol **189,** 275–284, 2001.
24. Mauck, R.L., Yuan, X., and Tuan, R.S. Chondrogenic differentiation and functional maturation of bovine mesenchymal

stem cells in long-term agarose culture. Osteoarthritis Cartilage **14,** 179–189, 2006.
25. Williams, C.G., Kim, T.K., Taboas, A., Malik, A., Manson, P., and Elisseeff, J. *In vitro* chondrogenesis of bone marrow-derived mesenchymal stem cells in a photopolymerizing hydrogel. Tissue Eng **9,** 679–688, 2003.
26. Erickson, G.R., Gimble, J.M., Franklin, D.M., Rice, H.E., Awad, H., and Guilak, F. Chondrogenic potential of adipose tissue-derived stromal cells *in vitro* and *in vivo*. Biochem Biophys Res Commun **290,** 763–769, 2002.
27. Awad, H.A., Wickham, M.Q., Leddy, H.A., Gimble, J.M., and Guilak, F. Chondrogenic differentiation of adipose-derived adult stem cells in agarose, alginate, and gelatin scaffolds. Biomaterials **25,** 3211–3222, 2004.
28. Caterson, E.J., Li, W.J., Nesti, L.J., Albert, T., Danielson, K., and Tuan, R.S. Polymer/alginate amalgam for cartilage-tissue engineering. Ann NY Acad Sci **961,** 134–138, 2002.
29. Huang, A.H., Yeger-McKeever, M., Stein, A., and Mauck, R.L. Identification of molecular antecedents limiting functional maturation of MSC-laden hydrogels. Trans of the 54th Annual Meeting of the Orthopaedic Research Society, San Francisco, CA, 2008.
30. Nuttelman, C.R., Tripodi, M.C., and Anseth, K.S. Synthetic hydrogel niches that promote hMSC viability. Matrix Biol **24,** 208–218, 2005.
31. Salinas, C.N., Cole, B.B., Kasko, A.M., and Anseth, K.S. Chondrogenic differentiation potential of human mesenchymal stem cells photoencapsulated within poly (ethylene glycol)-arginine-glycine-aspartic acid-serine thiol-methacrylate mixed-mode networks. Tissue Eng **13,** 1025–1034, 2007.
32. Kisiday, J., Jin, M., Kurz, B., Hung, H., Semino, C., Zhang, S., and Grodzinsky, A.J. Self-assembling peptide hydrogel fosters chondrocyte extracellular matrix production and cell division: implications for cartilage tissue repair. Proc Natl Acad Sci USA **99,** 9996–10001, 2002.
33. Kisiday, J.D., Kurz, B., DiMicco, M.A., and Grodzinsky, A.J. Evaluation of medium supplemented with insulin-transferrin-selenium for culture of primary bovine calf chondrocytes in three-dimensional hydrogel scaffolds. Tissue Eng **11,** 141–151, 2005.
34. Kisiday, J.D., Kopesky, P.W., Evans, C.H., Grodzinsky, A.J., McIlwraith, C.W., and Frisbie, D.D. Evaluation of adult equine bone marrow- and adipose-derived progenitor cell chondrogenesis in hydrogel cultures. J Orthop Res **26,** 322–331, 2008.
35. Mauck, R.L., Helm, J.M., and Tuan, R.S. Chondrogenesis of human MSCs in a 3D self-assembling peptide hydrogel: functional properties and divergent expression profiles compared to pellet cultures. Trans ORS **31,** 775, 2006.
36. Holmes, T.C., de Lacalle, S., Su, X., Liu, G., Rich, A., and Zhang, S. Extensive neurite outgrowth and active synapse formation on self-assembling peptide scaffolds. Proc Natl Acad Sci USA **97,** 6728–6733, 2000.
37. Nettles, D.L., Vail, T.P., Morgan, M.T., Grinstaff, M.W., and Setton, L.A. Photocrosslinkable hyaluronan as a scaffold for articular cartilage repair. Ann Biomed Eng **32,** 391–397, 2004.
38. Burdick, J.A., Chung, C., Jia, X., Randolph, M.A., and Langer, R. Controlled degradation and mechanical behavior of photopolymerized hyaluronic acid networks. Biomacromolecules **6,** 386–391, 2005.
39. Chung, C., Mesa, J., Miller, G.J., Randolph, M.A., Gill, T.J., and Burdick, J.A. Effects of auricular chondrocyte expansion on neocartilage formation in photocrosslinked hyaluronic acid networks. Tissue Eng **12,** 2665–2673, 2006.
40. Li, Y., Toole, B.P., Dealy, C.N., and Kosher, R.A. Hyaluronan in limb morphogenesis. Dev Biol **305,** 411–420, 2007.
41. Toole, B.P. Hyaluronan: from extracellular glue to pericellular cue. Nat Rev Cancer **4,** 528–539, 2004.
42. Knudson, C.B., and Knudson, W. Hyaluronan and CD44: modulators of chondrocyte metabolism. Clin Orthop Relat Res **427 suppl,** S152–S162, 2004.
43. Knudson, C.B. Hyaluronan receptor-directed assembly of chondrocyte pericellular matrix. J Cell Biol **120,** 825–834, 1993.
44. Morales, T.I., and Hascall, V.C. Correlated metabolism of proteoglycans and hyaluronic acid in bovine cartilage organ cultures. J Biol Chem **263,** 3632–3638, 1988.
45. Mauck, R.L., Wang, C.C., Oswald, E.S., Ateshian, G.A., and Hung, C.T. The role of cell seeding density and nutrient supply for articular cartilage tissue engineering with deformational loading. Osteoarthritis Cartilage **11,** 879–890, 2003.
46. Chung, C., Mesa, J., Randolph, M.A., Yaremchuk, M., and Burdick, J.A. Influence of gel properties on neocartilage formation by auricular chondrocytes photoencapsulated in hyaluronic acid networks. J Biomed Mater Res A **77,** 518–525, 2006.
47. Park, S.Y., Hung, C.T., and Ateshian, G.A. Mechanical response of bovine articular cartilage under dynamic unconfined compression loading at physiological stress levels. J Biomech **12,** 391–400, 2003.
48. Farndale, R.W., Buttle, D.J., and Barrett, A.J. Improved quantitation and discrimination of sulphated glycosaminoglycans by use of dimethylmethylene blue. Biochim Biophys Acta **883,** 173–177, 1986.
49. Stegemann, H., and Stalder, K. Determination of hydroxyproline. Clin Chim Acta **18,** 267–273, 1967.
50. Vunjak-Novakovic, G., Martin, I., Obradovic, B., Treppo, S., Grodzinsky, A.J., Langer, R., and Freed, L.E. Bioreactor cultivation conditions modulate the composition and mechanical properties of tissue-engineered cartilage. J Orthop Res **17,** 130–138, 1999.
51. Aufderheide, A.C., and Athanasiou, K.A. Assessment of a bovine co-culture, scaffold-free method for growing meniscus-shaped constructs. Tissue Eng **13,** 2195–2205, 2007.
52. Erickson, I.E., Chung, C., Burdick, J.A., and Mauck, R.L. Hyaluronic acid macromer concentration influences functional MSC chondrogenesis in photocrosslinked MSC-laden hydrogels. Proc BIO2008 Summer Bioengineering Conference, Marco Island, FL, 2008.
53. Sahoo, S., Chung, C., Khetan, S., and Burdick, J.A. Hydrolytically degradable hyaluronic acid hydrogels with controlled temporal network structures. Biomacromolecules **9,** 1088–1092, 2008.
54. Mauck, R.L., Seyhan, S.L., Ateshian, G.A., and Hung, C.T. Influence of seeding density and dynamic deformational loading on the developing structure/function relationships of chondrocyte-seeded agarose hydrogels. Ann Biomed Eng **30,** 1046–1056, 2002.
55. Huang, A.H., Yeger-McKeever, M., Stein, A., and Mauck, R.L. Tensile properties of engineered cartilage formed from chondrocyte and MSC-laden hydrogels. Osteoarthritis Cartilage **6,** 1074–1082, 2008.
56. Engler, A.J., Sen, S., Sweeney, H.L., and Discher, D.E. Matrix elasticity directs stem cell lineage specification. Cell **126,** 677–89, 2006.
57. Mauck, R.L., Soltz, M.A., Wang, C.C., Wong, D.D., Chao, P.H., Valhmu, W.B., Hung, C.T., and Ateshian, G.A.

Functional tissue engineering of articular cartilage through dynamic loading of chondrocyte-seeded agarose gels. J Biomech Eng **122,** 252–260, 2000.
58. Chung, C., Erickson, I.E., Mauck, R.L., and Burdick, J.A. Differential behavior of auricular and articular chondrocytes in hyaluronic acid hydrogels. Tissue Eng Part A **14,** 1121–1131, 2008.
59. Kisiday, J.D., Jin, M., DiMicco, M.A., Kurz, B., and Grodzinsky, A.J. Effects of dynamic compressive loading on chondrocyte biosynthesis in self-assembling peptide scaffolds. J Biomech **37,** 595–604, 2004.
60. Mauck, R.L., Byers, B.A., Yuan, X., and Tuan, R.S. Regulation of cartilaginous ECM gene transcription by chondrocytes and MSCs in 3D culture in response to dynamic loading. Biomech Model Mechanobiol **6,** 113–125, 2007.
61. Huang, C.Y., Hagar, K.L., Frost, L.E., Sun, Y., and Cheung, H.S. Effects of cyclic compressive loading on chondrogenesis of rabbit bone-marrow derived mesenchymal stem cells. Stem Cells **22,** 313–323, 2004.
62. Terraciano, V., Hwang, N., Moroni, L., Park, H.B., Zhang, Z., Mizrahi, J., Seliktar, D., and Elisseeff, J. Differential response of adult and embryonic mesenchymal progenitor cells to mechanical compression in hydrogels. Stem Cells **25,** 2730–2738, 2007.

Address reprint requests to:
Robert L. Mauck, Ph.D.
McKay Orthopaedic Research Laboratory
Department of Orthopaedic Surgery
University of Pennsylvania
424 Stemmler Hall
36th St. and Hamilton Walk
Philadelphia, PA 19104

E-mail: lemauck@mail.med.upenn.edu

Received: February 11, 2008
Accepted: July 8, 2008
Online Publication Date: December 30, 2008